*Hsuan-Teh Hu*[1]

# Buckling Analyses of Fiber-Composite Laminate Shells with Material Nonlinearity

**REFERENCE:** Hu, H.-T., **"Buckling Analyses of Fiber-Composite Laminate Shells with Material Nonlinearity,"** *Journal of Composites Technology & Research*, JCTRER, Vol. 15, No. 3, Fall 1993, pp. 202–208.

**ABSTRACT:** A nonlinear material constitutive model, including a nonlinear in-plane shear formulation and a failure criterion, for fiber-composite laminate materials is employed to carry out finite-element buckling analyses for composite shells under hydrostatic compressive loads. It has been shown that the nonlinear in-plane shear together with the failure criterion have significant influence on the buckling behavior of composite shells.

**KEYWORDS:** buckling, in-plane shear, constitutive model, failure criterion, composite shell

Due to the high stiffness-to-weight ratio, the use of fiber-reinforced composite materials in advanced shell structures, such as submarine pressure hulls, missile nozzles, aircraft fuselages, and satellite antennas, has increased rapidly in recent years. The composite shell structures are commonly subjected to various kinds of compressive loading, which may cause buckling. Therefore, knowledge of the buckling and postbuckling behavior of composite shells has become essential in design. In the literature, most stability studies of composite laminate shells have been limited to the geometrically nonlinear analysis [*1–3*]. Little attention has been paid to the material nonlinearity.

It is well known that unidirectional fibrous composites exhibit severe nonlinearity in in-plane shear stress-strain relation. In addition, deviation from linearity is also observed in in-plane transverse loadings but the degree of nonlinearity is not comparable to that in the in-plane shear [*4*]. For graphite/epoxy and boron/epoxy, this nonlinearity associated with the transverse loadings can usually be ignored [*5*].

A significant number of macromechanical models have been proposed to represent the constitutive relation of fiber-composite materials such as nonlinear elasticity models [*4,6,7*], or plasticity models [*8–11*]. In addition, various failure criteria have also been proposed to predict the onset of failure in single layer of fiber-reinforced composites, such as the maximum strain theory, maximum stress theory, Tsai-Wu theory, Hoffman theory, etc. [*12*]. The mechanical response of fiber-composite materials is very complicated. Since the nonlinearity of the in-plane shear is significant for composite materials, this work is therefore focusing on the influence of the in-plane shear nonlinearity together with a failure criterion on the buckling response of composite shells.

In this paper, a material model including the nonlinear in-plane shear and the Tsai-Wu failure criterion is reviewed first. Then, buckling analyses with this nonlinear material model for simply supported composite shells under hydrostatic compression are carried out using the ABAQUS finite element program [*13*]. Numerical results for the material nonlinear buckling behavior of these composite shells are compared with those using linear material properties. Finally, important conclusions obtained from this study are given.

## Constitutive Modeling of Single Lamina

For fiber-composite laminate materials, each lamina can be considered as an orthotropic layer in a plane stress condition. The incremental constitutive matrices for a linear orthotropic lamina in the material coordinates (Fig. 1) can be written as

$$\Delta\{\sigma'\} = [Q_1']\Delta\{\varepsilon'\} \tag{1}$$

$$\Delta\{\tau_t'\} = [Q_2']\Delta\{\gamma_t'\} \tag{2}$$

where $\Delta\{\sigma'\} = \Delta\{\sigma_1, \sigma_2, \tau_{12}\}^T$, $\Delta\{\tau_t'\} = \Delta\{\tau_{13}, \tau_{23}\}^T$, $\Delta\{\varepsilon'\} = \Delta\{\varepsilon_1, \varepsilon_2, \gamma_{12}\}^T$, $\Delta\{\gamma_t'\} = \Delta\{\gamma_{13}, \gamma_{23}\}^T$ are incremental stress and strain components, and

$$[Q_1'] = \begin{bmatrix} \dfrac{E_{11}}{1-\nu_{12}\nu_{21}} & \dfrac{\nu_{12}E_{22}}{1-\nu_{12}\nu_{21}} & 0 \\ \dfrac{\nu_{21}E_{11}}{1-\nu_{12}\nu_{21}} & \dfrac{E_{22}}{1-\nu_{12}\nu_{21}} & 0 \\ 0 & 0 & G_{12} \end{bmatrix} \tag{3}$$

$$[Q_2'] = \begin{bmatrix} \alpha_1 G_{13} & 0 \\ 0 & \alpha_2 G_{23} \end{bmatrix} \tag{4}$$

where $\alpha_1$ and $\alpha_2$ are the shear correction factors [*14*] and are taken to be 5/6 in this study.

To model the nonlinear in-plane shear behavior, the nonlinear

[1]Associate professor, Department of Civil Engineering, National Cheng Kung University, Tainan, Taiwan 70101, R.O.C.

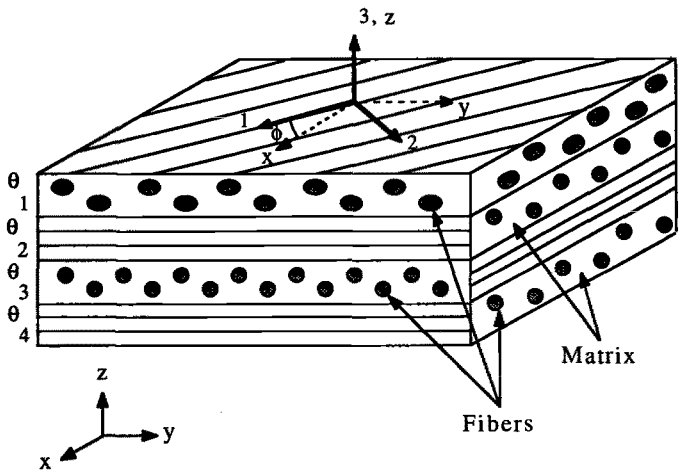


FIG. 1—*Material and element coordinate systems for fiber composite laminate.*

strain-stress relation for a composite lamina suggested by Hahn and Tsai [*4*] is adopted in this study, which is given as follows:

$$\begin{Bmatrix} \varepsilon_1 \\ \varepsilon_2 \\ \gamma_{12} \end{Bmatrix} = \begin{bmatrix} \frac{1}{E_{11}} & -\frac{\nu_{21}}{E_{22}} & 0 \\ -\frac{\nu_{12}}{E_{11}} & \frac{1}{E_{22}} & 0 \\ 0 & 0 & \frac{1}{G_{12}} \end{bmatrix} \begin{Bmatrix} \sigma_1 \\ \sigma_2 \\ \tau_{12} \end{Bmatrix} + S_{6666}\tau_{12}^2 \begin{Bmatrix} 0 \\ 0 \\ \tau_{12} \end{Bmatrix} \quad (5)$$

In this equation only one material constant $S_{6666}$ is required to account for the in-plane shear nonlinearity. The value of $S_{6666}$ can be determined by a curve fit to various off-axis tension test data [*4*]. By inverting and differentiating Eq 5, the nonlinear incremental constitutive matrix for the lamina becomes

$$[Q_1'] = \begin{bmatrix} \frac{E_{11}}{1-\nu_{12}\nu_{21}} & \frac{\nu_{12}E_{22}}{1-\nu_{12}\nu_{21}} & 0 \\ \frac{\nu_{21}E_{11}}{1-\nu_{12}\nu_{21}} & \frac{E_{22}}{1-\nu_{12}\nu_{21}} & 0 \\ 0 & 0 & \frac{1}{1/G_{12} + 3S_{6666}\tau_{12}^2} \end{bmatrix} \quad (6)$$

### Failure Criterion and Degradation of Stiffness

Among existing failure criteria, the Tsai-Wu criterion [*15*] has been extensively used in literature and it is adopted in this analysis. Under plane stress conditions, this failure criterion has the following form

$$F_1\sigma_1 + F_2\sigma_2 + F_{11}\sigma_1^2 + 2F_{12}\sigma_1\sigma_2 + F_{22}\sigma_2^2 + F_{66}\sigma_{12}^2 = 1 \quad (7)$$

where

$$F_1 = \frac{1}{X} + \frac{1}{X'}, F_2 = \frac{1}{Y} + \frac{1}{Y'}, F_{11} = \frac{-1}{XX'},$$

$$F_{22} = \frac{-1}{YY'}, F_{66} = \frac{1}{S^2}$$

The $X$, $Y$ and $X'$, $Y'$ are the lamina longitudinal and transverse strengths in tension and compression, respectively, and $S$ is the shear strength of the lamina. Though the stress interaction term $F_{12}$ in Eq 7 is difficult to be determined, it has been suggested by Narayanaswami and Adelman [*16*] that $F_{12}$ can be set equal to zero for practical engineering applications. Therefore, $F_{12} = 0$ is used in this investigation.

During the numerical calculation, incremental loading is applied to composite shells until failure in one or more of the individual plies is indicated according to Eq 7. Since the Tsai-Wu criterion does not distinguish failure modes, the following two rules are used to determine whether the ply failure is caused by resin fracture or fiber breakage [*12*]:

(1) If a ply fails but the stress in the fiber direction remains less than the uniaxial strength of the lamina in the fiber direction, i.e. $X' < \sigma_1 < X$, the ply failure is assumed to be resin induced. Consequently, the laminate loses its capability to support transverse and shear stresses, but remains to carry longitudinal stress. Under this condition, the degraded constitutive matrix of a composite lamina becomes:

$$[Q_1'] = \begin{bmatrix} E_{11} & 0 & 0 \\ 0 & 0 & 0 \\ 0 & 0 & 0 \end{bmatrix} \quad (8)$$

(2) If a ply fails with $\sigma_1$ exceeding the uniaxial strength of the lamina, the ply failure is caused by fiber breakage and total ply rupture is assumed. Under this condition, the degraded constitutive matrix of a composite lamina becomes:

$$[Q_1'] = \begin{bmatrix} 0 & 0 & 0 \\ 0 & 0 & 0 \\ 0 & 0 & 0 \end{bmatrix} \quad (9)$$

### Constitutive Modeling of Composite Shell Section

The elements used in the finite-element analyses are eight-node isoparametric shell elements with six degrees of freedom per node (three displacements and three rotations). The formulation of the shell allows transverse shear deformation [*13,17*] and these shear flexible shells can be used for both thick and thin shell analysis [*13*].

During a finite element analysis, the constitutive matrix of composite materials at the integration points of shell elements must be calculated before the stiffness matrices are assembled from the element level to the structural level. For fiber-composite laminate materials, the incremental constitutive equations of a lamina in the element coordinates ($x$, $y$, $z$) can be written as

$$\Delta\{\sigma\} = [Q_1]\Delta\{\varepsilon\} \quad (10)$$

$$\Delta\{\tau_i\} = [Q_2]\Delta\{\gamma_i\} \quad (11)$$

where $\Delta\{\sigma\} = \Delta\{\sigma_x, \sigma_y, \tau_{xy}\}^T$, $\Delta\{\tau_t\} = \Delta\{\tau_{xz}, \tau_{yz}\}^T$, $\Delta\{\varepsilon\} = \Delta\{\varepsilon_x, \varepsilon_y, \gamma_{xy}\}^T$, $\Delta\{\gamma_t\} = \Delta\{\gamma_{xz}, \gamma_{yz}\}^T$,

$$[Q_1] = [T_1]^T[Q_1'][T_1] \tag{12}$$

$$[Q_2] = [T_2]^T[Q_2'][T_2] \tag{13}$$

$$[T_1] = \begin{bmatrix} \cos^2\phi & \sin^2\phi & \sin\phi\cos\phi \\ \sin^2\phi & \cos^2\phi & -\sin\phi\cos\phi \\ -2\sin\phi\cos\phi & 2\sin\phi\cos\phi & \cos^2\phi - \sin^2\phi \end{bmatrix} \tag{14}$$

$$[T_2] = \begin{bmatrix} \cos\phi & \sin\phi \\ -\sin\phi & \cos\phi \end{bmatrix} \tag{15}$$

and $\phi$ is measured counterclockwise from the element local $x$-axis to the material 1-axis.

Assume $\Delta\{\varepsilon_o\} = \Delta\{\varepsilon_{xo}, \varepsilon_{yo}, \gamma_{xyo}\}^T$ are the incremental in-plane strains at the mid-surface of the section and $\Delta\{\kappa\} = \Delta\{\kappa_x, \kappa_y, \kappa_{xy}\}^T$ are the incremental curvatures. The incremental in-plane strains at a distance $z$ from the mid-surface of the shell section become

$$\Delta\{\varepsilon\} = \Delta\{\varepsilon_o\} + z\Delta\{\kappa\} \tag{16}$$

Let $h$ be the total thickness of the shell section, the incremental stress resultants, $\Delta\{N\} = \Delta\{N_x, N_y, N_{xy}\}^T$, $\Delta\{M\} = \Delta\{M_x, M_y, M_{xy}\}^T$ and $\Delta\{V\} = \Delta\{V_x, V_y\}$, can be defined as

$$\begin{Bmatrix} \Delta\{N\} \\ \Delta\{M\} \\ \Delta\{V\} \end{Bmatrix} = \int_{-h/2}^{h/2} \begin{Bmatrix} \Delta\{\sigma\} \\ z\Delta\{\sigma\} \\ \Delta\{\tau_t\} \end{Bmatrix} dz$$

$$= \int_{-h/2}^{h/2} \begin{Bmatrix} [Q_1](\Delta\{\varepsilon_o\} + z\Delta\{\kappa\}) \\ z[Q_1](\Delta\{\varepsilon_o\} + z\Delta\{\kappa\}) \\ [Q_2]\Delta\{\gamma_t\} \end{Bmatrix} dz$$

$$= \int_{-h/2}^{h/2} \begin{bmatrix} [Q_1] & z[Q_1] & [0] \\ z[Q_1] & z^2[Q_1] & [0] \\ [0]^T & [0]^T & [Q_2] \end{bmatrix} \begin{Bmatrix} \Delta\{\varepsilon_o\} \\ \Delta\{\kappa\} \\ \Delta\{\gamma_t\} \end{Bmatrix} dz \tag{17}$$

where [0] is a 3 by 2 matrix with all the coefficients equal to zero.

For the nonlinear material case, the $[Q_1']$ matrix in Eq 12 can be taken from Eqs 6, 8, or 9 and the incremental stress resultants of Eq 17 can be obtained by a numerical integration through the thickness of the composite shell section. For the linear material case, the $[Q_1']$ matrix used in Eq 12 is taken from Eq 3 and the incremental stress resultants of the shell section can be written as a summation of integrals over the $n$ laminae in the following form

$$\begin{Bmatrix} \Delta\{N\} \\ \Delta\{M\} \\ \Delta\{V\} \end{Bmatrix} = \left( \sum_{j=1}^{n} \begin{bmatrix} (z_{jt} - z_{jb})[Q_1] & \frac{1}{2}(z_{jt}^2 - z_{jb}^2)[Q_1] & [0] \\ \frac{1}{2}(z_{jt}^2 - z_{jb}^2)[Q_1] & \frac{1}{3}(z_{jt}^3 - z_{jb}^3)[Q_1] & [0] \\ [0]^T & [0]^T & (z_{jt} - z_{jb})[Q_2] \end{bmatrix} \right) \begin{Bmatrix} \Delta\{\varepsilon_o\} \\ \Delta\{\kappa\} \\ \Delta\{\gamma_t\} \end{Bmatrix} \tag{18}$$

where $z_{jt}$ and $z_{jb}$ are distances from the mid-surface of the section to the top and the bottom of the $j$-th layer, respectively.

## Nonlinear Finite Element Analysis

In the ABAQUS finite element program, the nonlinear response of a structure is modeled by an updated Lagrangian formulation and a modified Riks nonlinear incremental algorithm [*18*] can be used to construct the equilibrium solution path. To model bifurcation from the prebuckling path to the postbuckling path, geometric imperfections of composite shells are introduced by superimposing a small fraction (say, 0.001 of the shell thickness) of the lowest eigenmode determined by a linearized buckling analysis to the original nodal coordinates of shells.

## Numerical Analyses

### *Composite Shells with $[90/0]_{2S}$ and $[45/-45]_{2S}$ Layups*

In this section, fiber-composite laminate cylindrical shells with two laminate layups, $[90/0]_{2S}$ and $[45/-45]_{2S}$, are analyzed. The thickness of each ply is 1.02 mm. The material used for the analysis is graphite epoxy. Ply constitutive properties and shell geometries are given in Fig. 2. The linear and nonlinear in-plane shear stress-strain curves for a typical lamina are shown in Fig. 3. Both shells are subjected to uniform hydrostatic compression in the radial and axial directions. The ends of the shells are simply supported, which prevents radial motions but allows movements in axial direction. In addition, displacement constraints are enforced at the ends so that each point on the end of the cylinder, around the circumference, displaces axially the same amount. In the numerical analysis, the entire shell is modeled by 100 shell elements. The pressure applied at the closed end surfaces are transformed into equivalent ring loads applied at the edges.

To estimate the buckling loads and to generate geometric imperfections for composite shells, linearized buckling analyses are carried out first. The linearized buckling loads and buckling modes are shown in Fig. 4. It can be seen that the buckling modes of the composite shells are sensitive to laminate layups.

The load-displacement curves for the shell with a $[90/0]_{2S}$ layup are plotted in Fig. 5. The vertical axis is the hydrostatic pressure (positive value means compression) applied to the shell and the horizontal axis is the end displacement (positive value means end extension and negative value means end shortening). It can be seen that the behaviors of the shell predicted by using the linear and the nonlinear in-plane shear formulations are almost the same in the prebuckling stage. However, the postbuckling strength of the shell calculated using the nonlinear in-plane shear formulation is much lower than that calculated using the linear in-plane shear formulation. For the analysis carried out using the nonlinear in-plane shear formulation together with the Tsai-Wu criterion, the composite shell fails immediately after the buckling of shell occurs. The computed failure load is very close to the linearized buckling load.

Figure 6 plots the load-displacement curves for the shell with a $[45/-45]_{2S}$ layup. With this kind of laminate layup, each lamina in the composite shell is subjected to severe shear loading. Therefore, it is a good sample to test the influence of nonlinear in-plane shear and failure theory on the buckling behavior of the shell. For the analysis carried out using the linear shear formulation, the shell exhibits end extension before buckling occurs. However, after buckling takes place, the amount of end exten-

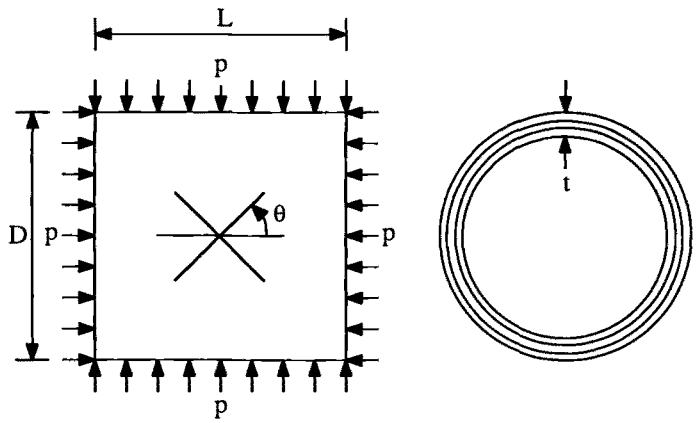


Laminate layups:
$[90/0]_{2S}$
$[45/-45]_{2S}$

Ply constitutive properties:
$E_{11}$ = 138 GPa
$E_{22}$ = 14.5 GPa
$G_{12} = G_{13}$ = 5.86 GPa
$G_{23}$ = 3.52 GPa
$\nu_{12}$ = 0.21
$S_{6666}$ = 7.31 $(GPa)^{-3}$

Shell geometry:
L = 20.32 cm
D = 20.32 cm
t = 0.81 cm

Ply strengths:
X = 1450 MPa
X' = -1450 MPa
Y = 52 MPa
Y' = -206 MPa
S = 93 MPa

FIG. 2—*Geometric and material properties for graphite/epoxy composite laminate shell.*

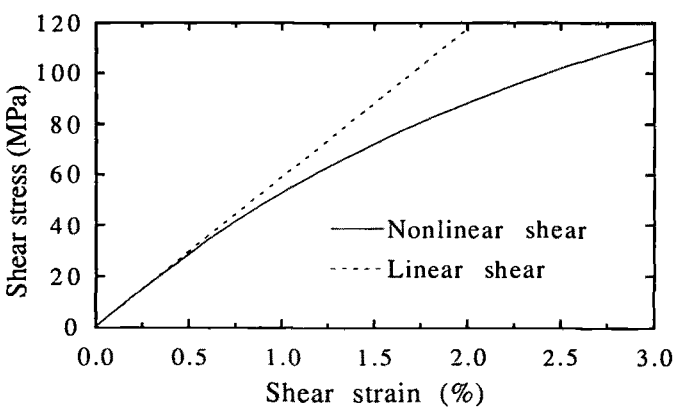


FIG. 3—*In-plane shear stress-strain curves for composite lamina.*

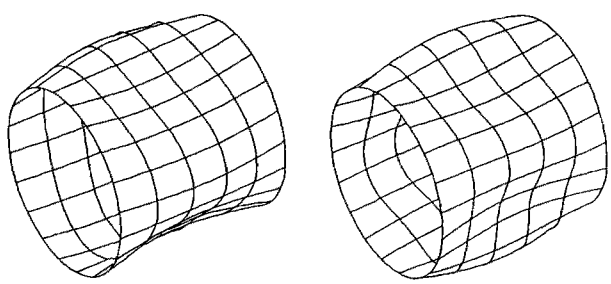

$p_{cr}$ = 44.8 MPa
$[90/0]_{2S}$ layup

$p_{cr}$ = 50.9 MPa
$[45/-45]_{2S}$ layup

FIG. 4—*Critical buckling loads and buckling modes for composite shells under hydrostatic compression.*

sion starts to reduce. For the analysis with the nonlinear in-plane shear formulation alone, the shell exhibits very nonlinear behavior throughout the entire loading stage. The stiffness and the load carrying capacity for the shell with the nonlinear in-plane shear formulation are much less than those with the linear shear formulation. For the analysis carried out using the nonlinear in-plane shear formulation together with the Tsai-Wu criterion, the shell exhibits a sudden failure mode while the loading is very low. The predicted failure strength of the composite shell is only about 62% of the linearized buckling load.

*Composite Shells with* $[\pm\theta/90/0]_S$ *Layups*

In this section, the $[\pm\theta/90/0]_S$ composite laminate shells are analyzed. The geometric and material properties, loading, and finite element mesh of the shells are the same as those in the previous section.

Figures 7 to 13 show the load-displacement curves, computed using the nonlinear in-plane shear formulation together with the Tsai-Wu criterion, for composite shells with various θ angles. For shells with θ angles equal to 0°, 30°, 60°, and 90° (i.e., Figs.

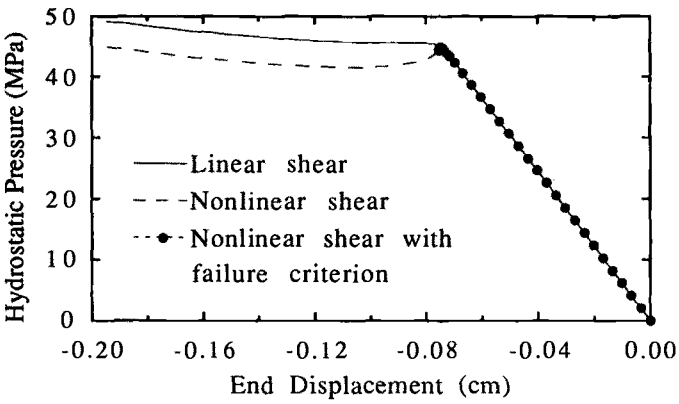


FIG. 5—*Load-displacement curves for composite shell with* $[90/0]_{2S}$ *layup under hydrostatic compression.*

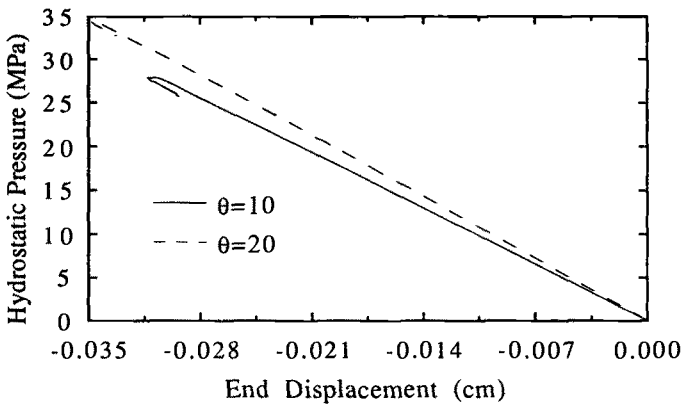


FIG. 8—*Load displacement curves for composite shells with* $[\pm 10/90/0]_S$ *and* $[\pm 20/90/0]_S$ *layups under hydrostatic compression (nonlinear shear with failure criterion only).*

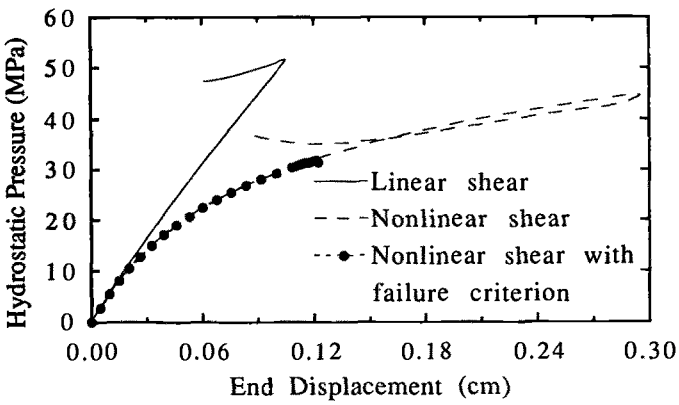


FIG. 6—*Load-displacement curves for composite shell with* $[45/-45]_{2S}$ *layup under hydrostatic compression.*

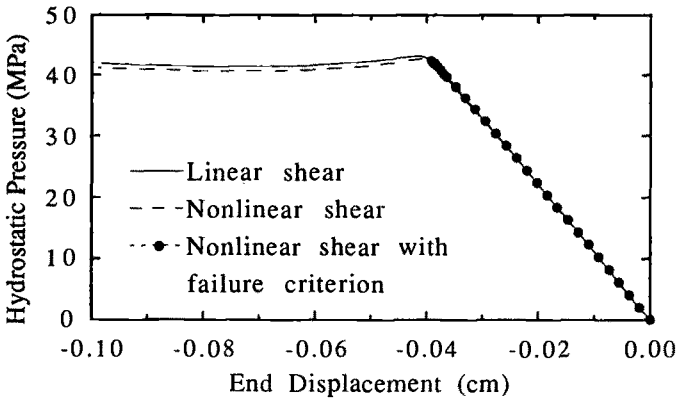


FIG. 9—*Load-displacement curves for composite shell with* $[\pm 30/90/0]_S$ *layup under hydrostatic compression.*

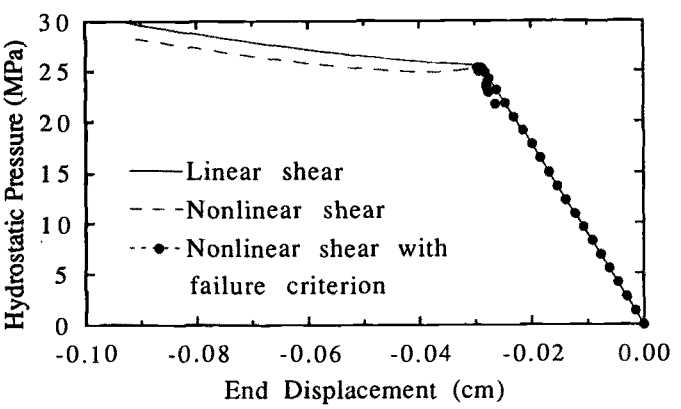


FIG. 7—*Load-displacement curves for composite shell with* $[\pm 0/90/0]_S$ *layup under hydrostatic compression.*

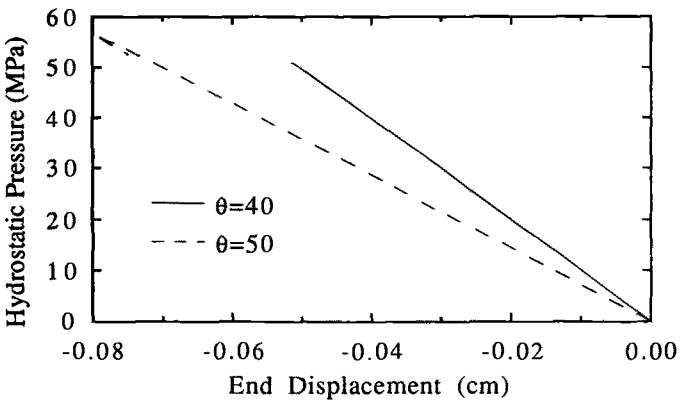


FIG. 10—*Load-displacement curves for composite shells with* $[\pm 40/90/0]_S$ *and* $[\pm 50/90/0]_S$ *layups under hydrostatic compression (nonlinear shear with failure criterion only).*

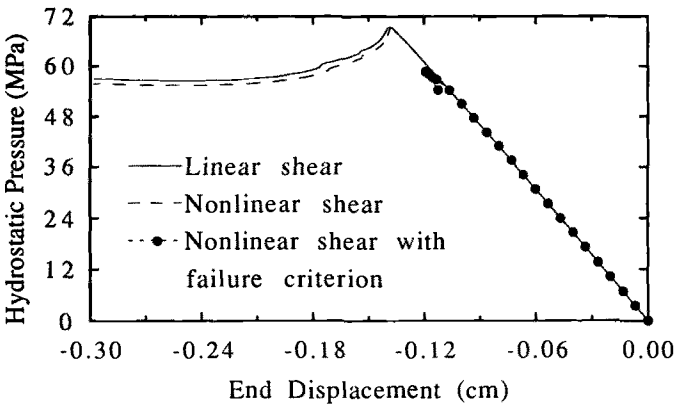


FIG. 11—*Load-displacement curves for composite shell with* $[\pm 60/90/0]_S$ *layup under hydrostatic compression.*

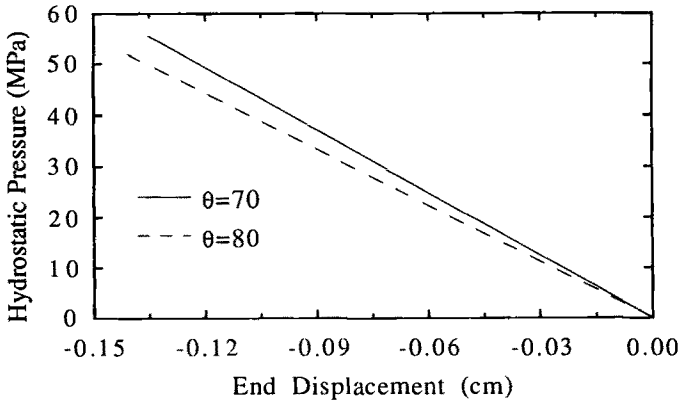


FIG. 12—*Load-displacement curves for composite shells with* $[\pm 70/90/0]_S$ *and* $[\pm 80/90/0]_S$ *layups under hydrostatic compression (nonlinear shear with failure criterion only).*

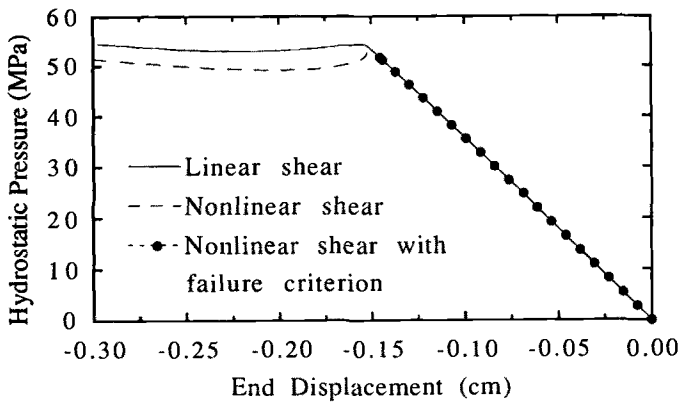


FIG. 13—*Load-displacement curves for composite shell with* $[\pm 90/90/0]_S$ *layup under hydrostatic compression.*

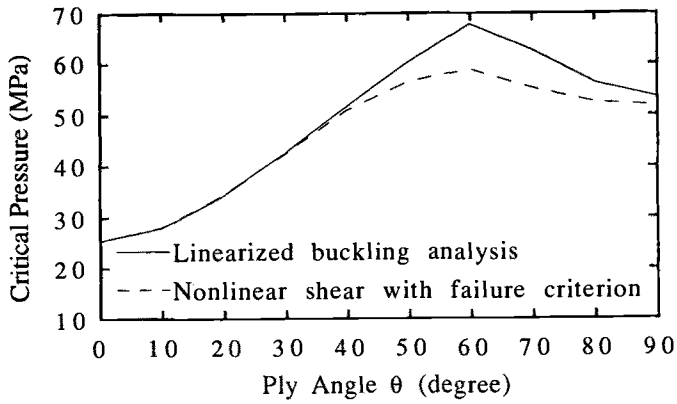


FIG. 14—*Critical load* $p_{cr}$ *as a function of* θ *for composite shells with* $[\pm\theta/90/0]_S$ *layup under hydrostatic compression.*

7, 9, 11, and 13), additional load-displacement curves computed using the linear and nonlinear in-plane shear formulations are also plotted.

From Figs. 7, 9, 11, and 13, one can see that the nonlinear in-plane shear alone has very little influence on the prebuckling response and the buckling strength of these shells. However, its influence on the postbuckling responses of these shells depends on the θ angle. For instance, when θ angle is equal to 0° or 90° (Figs. 7 and 13), the influence of nonlinear in-plane shear on the postbuckling response of the shell is significant. On the other hand, when θ angle is equal to 30° or 60° (Figs. 9 and 11), the influence of nonlinear in-plane shear on the postbuckling response of the shell is little.

For the analysis carried out using the nonlinear in-plane shear formulation together with the Tsai-Wu criterion, all the composite shells exhibit sudden failure before or immediately after the buckling occurs (Figs. 7 to 13). In Fig. 14 the predicted ultimate strengths of the composite shells using the nonlinear shear formulation together with the Tsai-Wu criterion are compared with those obtained by the linearized buckling analyses. From this figure, one can see that the predicted ultimate strengths of the shells with θ between 0° and 40° and with θ close to 90° are very close to the linearized buckling loads. On the other hand, the predicted ultimate strengths of the shells with θ between 50° and 80° are much lower than the linearized buckling loads. It can also be observed that the optimal fiber angle θ for the shells with the material nonlinear analysis is very close to the optimal fiber angle for the shells with linearized buckling analysis, which is about 60° for both cases.

## Conclusions

For the material nonlinear analysis of composite shells with various laminate layups and subjected to hydrostatic compression, the following conclusions can be drawn:

(1) The nonlinear in-plane shear alone has very little influence on the prebuckling response and the buckling strengths of the shells with $[90/0]_{2S}$ and $[\pm\theta/90/0]_S$ layups. However, its effect on the reduction of postbuckling strengths of these shells depends on the laminate layups.

(2) The nonlinear in-plane shear together with material failure according to the Tsai-Wu failure theory has very little influence on the prebuckling stiffnesses of the shells with $[90/0]_{2S}$ and $[\pm\theta/90/0]_S$ layups. However, its effect on the reduction of ultimate

strengths of these shells depends on the laminate layups. In addition, these shells exhibit sudden failure before or immediately after the buckling occurs.

(3) The nonlinear in-plane shear alone has significant influence on the prebuckling response as well as the postbuckling response of the shell with a $[45/-45]_{2S}$ layup. In addition, if the Tsai-Wu criterion is considered, the predicted ultimate strength of the composite shell is much lower than the linearized buckling load and the shell exhibits a sudden failure mode.

*Acknowledgment*

The author wishes to express his appreciation to Dr. Su Su Wang, the Distinguished University Professor of the University of Houston, Texas, for his encouragement and fruitful discussion during the early stage of this study. This work was financially supported by the National Science Council of the Republic of China under Grant NSC 82-0401-E-006-374.

## References

[1] Leissa, A. W., "Buckling of Laminated Plates and Shell Panels," *Technical Report AFWAL-TR-85-3069*, Air Force Wright Aeronautical Laboratories, Wright-Patterson Air Force Base, OH, 1985.

[2] Knight, N. F. and Starnes, J. H., "Postbuckling Behavior of Axially Compressed Graphite-Epoxy Cylindrical Panels with Circular Holes," *Journal of Pressure Vessel Technology, ASME*, Vol. 107, 1985, pp. 394–402.

[3] Hong, C. S. and Jun, S. M., "Buckling Behavior of Laminated Composite Cylindrical Panels under Axial Compression," *Computers and Structures*, Vol. 29, 1988, pp. 479–490.

[4] Hahn, H. T. and Tsai, S. W., "Nonlinear Elastic Behavior of Unidirectional Composite Laminae," *Journal of Composite Materials*, Vol. 7, 1973, pp. 102–118.

[5] Jones, R. M. and Morgan, H. S., "Analysis of Nonlinear Stress-Strain Behavior of Fiber-Reinforced Composite Materials," *AIAA Journal*, Vol. 15, 1977, pp. 1669–1676.

[6] Hashin, Z., Bagchi, D., and Rosen, B. W., "Non-Linear Behavior of Fiber Composite Laminates," *NASA Contractor Report*, NASA CR-2313, 1974.

[7] Hajali, R. and Wang, S. S., "Nonlinear Behavior of Fiber Composite Materials and Its Effect on the Postbuckling Response of Laminated Plates," *Technical Report UIUC-NCCMR-90-10*, National Center for Composite Materials Research, University of Illinois, Urbana, IL, 1990.

[8] Sun, C. T. and Chen, J. L., "A Simple Flow Rule for Characterizing Nonlinear Behavior of Fiber Composites," *Journal of Composite Materials*, Vol. 23, 1989, pp. 1009–1020.

[9] Vaziri, R., Olson, M. D., and Anderson, D. L., "A Plasticity-Based Constitutive Model for Fibre-Reinforced Composite Laminates," *Journal of Composite Materials*, Vol. 25, 1991, pp. 512–535.

[10] Nanda, A. and Kuppusamy, T., "Three-Dimensional Elastic-Plastic Analysis of Laminated Composite Plates," *Composite Structures*, Vol. 17, 1991, pp. 213–225.

[11] Arnold, R. R. and Mayers, J., "Buckling, Postbuckling, and Crippling of Materially Nonlinear Composite Plates," *International Journal of Solids and Structures*, Vol. 20, 1984, pp. 863–880.

[12] Rowlands, R. E., "Strength (Failure) Theories and Their Experimental Correlation," *Failure Mechanics of Composites*, G. C. Sih and A. M. Skudra, Eds., Elsevier Science Publishers, The Netherlands, 1985, pp. 71–125.

[13] Hibbitt, Karlsson, and Sorensen, Inc., *ABAQUS User Manual*, Version 4-8, Providence, RI, 1991.

[14] Mindlin, R. D., "Influence of Rotatory Inertia and Shear on Flexural Motions of Isotropic, Elastic Plates," *Journal of Applied Mechanics*, Vol. 18, 1951, pp. 31–38.

[15] Tsai, S. W. and Wu, E. M., "A General Theory of Strength for Anisotropic Materials," *Journal of Composite Materials*, Vol. 5, 1971, pp. 58–80.

[16] Narayanaswami, R. and Adelman, H. M., "Evaluation of the Tensor Polynomial and Hoffman Strength Theories for Composite Materials," *Journal of Composite Materials*, Vol. 11, 1977, pp. 366–377.

[17] Irons, B. M., "The Semi-Loof Shell Element," *Finite Elements for Thin Shells and Curved Members*, D. G. Ashwell and R. H. Gallagher, Eds., John Wiley and Sons, London, U.K., 1976, pp. 197–222.

[18] Riks, E., "An Incremental Approach to the Solution of Snapping and Buckling Problems," *International Journal of Solids and Structures*, Vol. 15, 1979, pp. 529–551.